The Conference Paper Title is in Arial Bold 18pt

The Authors' Names are in Arial Bold 9.5pt
The Authors' Affiliations are in Arial Italic 9.5pt

Authors with a Second Affiliation go here
The Second Affiliation goes here (etc.)

Abstract. The abstract and keywords are in 9.5pt Arial and justified both sides. The abstract contains no more than **200** words. **The entire document, including all sections and figures, should not exceed 4 pages-long.** Submitted Conference Papers that do not comply with the guidelines and this template will be returned to the authors without being reviewed.

1 The Section Headings are Arial Bold 11pt (Heading 1)

The main text is in 9.5pt Arial. It is double justified with single line spacing. Do not indent the first lines of the first paragraphs within sections. *Use the inbuilt styles to make your task easier!*

Second and subsequent paragraphs are indented like this (Normal Indent style). Do not skip lines or use extended line breaks below paragraphs.

The page size is **Letter (North American standard – please do not convert this template to A4 or any other format) with 2 cm margins on all sides.** The columns are 8.4 cm wide and the space between the columns in the main text is 8 mm.

See **specimen abstract below** for examples of correct practice.

2 The Second Section Starts Like This

2.1 Subheadings work like this and are Arial Bold 10pt (Heading 2)

Use an empty line (Normal Style) to separate headings from the text.

Figure 1. Table and Figure captions use 8pt Arial. Table captions should be above table, figure captions below figure. Number sequentially through paper. Keep to column width of 8.4 cm. Exceptionally figures could span the page width.

Acknowledgements

Acknowledgments go after the main text and before the references.

References

The references are in 8pt Arial with a hanging indent (Reference List Style) See instructions for authors and the specimen abstract for formatting requirements.

All references have a hanging indent so that the first author stands out.

Referencing must comply with Mineralium Deposita standards and guidelines: **https://e-sga.org/publications/mineralium-deposita/instructions-for-authors/**

EXAMPLE - modified from Jenkin et al. (2017) in Proceedings of the 14th SGA Biennial Meeting, Quebec City, Canada.

An early magmatic fluid pulse at Cononish orogenic gold deposit? Tellurium enrichment and implications for orogenic gold formation

Title – justified not centred
Capital letters only for first word, abbreviations and formal names

Gawen R.T. Jenkin
University of Leicester

Carl Spence–Jones
University of Leeds

Adrian J. Boyce
Scottish Universities Environmental Research Centre

Nyree J. Hill, Christopher J.S. Sangster
Scotgold Resources

First name in full, initial(s) if applicable, and last name.
Affiliation sufficient, address unnecessary

Authors should be listed in order according to relative contribution, not by affiliation.
Where two fall together in adjacent order they can be clumped like this.
For a long complex author list the authors can have numbers that relate to a numbered affiliation list below.

No keywords

Abstract. Tellurium enrichment occurs in ma gold deposits. Fractionation of Te from Se offer insight into source/pathway processes fluids. In the Te–rich metasedimentary–hosted Cononish vein gold deposit, Scotland, Ag in Au–Ag alloy increases from ~20 to 80 wt.% through the paragenesis, correlating with decreasing hessite abundance. This suggests the Au–Ag a lled by the fluid Te activity, e. This is coupled to an incre to +11.4‰ through the paragenesis. Thus, the deposit formed from a primary fluid with a low– δ^{34}S and high Te+Au+Ag that evolved towards a high δ^{34}S–low Te fluid. The high δ^{34}S of the later fluid suggests it can only be a metamorphic fluid sourced from nearby SEDEX horizons. The early fluid that deposited most of the gold could be metamorphic fluid from other units in the stratigraphy, or magmatic in origin. Two observations taken together suggest it is most likely that this fluid was magmatic; the age of the mineralisation is identical to the last stage of crystallization of nearby granite batholiths, and the fluid has a S–isotope signature consistent with a magmatic source. Tellurium in *some* orogenic gold deposits may relate to magmatic input.

Abstract left aligned
200 words max

1 Introduction

Heading 1 Style

Orogenic gold deposits are a broad class of deposits exhibiting a common set of features (Goldfarb et al. 2005) and are typically deposited from low–salinity CO_2–bearing fluids (Goldfarb and Groves 2015). Despite commonality of broad features, variations in isotopic composition, mineral assemblage, and metal enrichments exist (Chapman and Mortensen 2016; Goldfarb and Groves 2015; Groves et al. 1998), and the interpreted source of the ore fluids, and the dissolved constituents they transport, remains controversial (Goldfarb et al. 2005; Goldfarb and Groves 2015; Wyman et al. 2016). Whilst a metamorphic fluid source remains the most likely model for the majority of orogenic deposits, input of magmatic fluids may be important in some deposits (Goldfarb et al. 2005). The cause of Te–

NO comma , in text citations – as in Mineralium Deposita

1989) whereas others suggest it need not (Goldfarb et al. 2000).

The planned development of the Cononish gold mine, Scotland (estimated reserves of 555,000 tonnes of ore grading at 11.1 g/t Au and 47.7 g/t Ag; Scotgold Resources l evelopment of Curraghinalt Ireland, has catalysed a genesis in the Caledonides ed 3 km south west of Ty e (Te/Au by weight ~≥1, suggesting >7 t Te; Science and Technology Committee 2011) and provides an excellent system in which to study the fluids and processes that formed the mineralisation. Fluid inclusion and stable isotope data are available, along with textural and mineralogical descriptions of the mineralised veins (Pattrick et al. 1988; Earls et al. 1992; Curtis et al. 1993). However, the detailed paragenesis of the veins has never been described and linked to mineral chemistry and stable isotope data. Furthermore, the genesis of the deposit remains contentious, with either magmatic or metamorphic fluids (±meteoric) interpreted to have formed the deposit (Pattrick et al. 1988; Curtis et al. 1993; Craw and Chamberlain 1996). Here, a combined study of the paragenesis, Au–Ag alloy composition, and sulfur isotopes provides evidence for an early Te–bearing magmatic fluid.

Numbers should be metric (or imperial + metric)

2 Geological setting

First paragraph of section is aligned to left (normal style)

The Tyndrum area comprises Neoproterozoic Dalradian Supergroup metasediments that were subjected to amphibolite–grade metamorphism and deformation (D_1–D_4) during the Grampian Orogeny, ~470 Ma (Stephenson et al. 2013). The sequence is dissected by major NE–trending sinistral faults with a normal component that developed late in the orogeny, including the Tyndrum fault. The Cononish deposit comprises a composite vein structure hosted within the sub–vertical Eas Anie

DO NOT insert page numbers

Structure (041/89SE) that is associated with a splay off the Tyndrum Fault (see geological map in Hill et al. 2013).

The Eas Anie Structure crosscuts Grampian and lower–Appin Group units that were deformed into large north–east verging nap[illegible] orogeny (Tanner and T[illegible] Cononish deposit is s[illegible] dipping limb of an antic[illegible] limb of the fold is overtu[illegible] below the deposit (Ear[illegible] 2013; Tanner 2014). The Cononish Au–Ag (±Cu, Pb) mineralisation was dated by Rice et al. (2012) at 408 ± 2 Ma and 407 ± 1 Ma using Ar/Ar of K–feldspar.

Second and subsequent paragraphs of section are indented like this (Normal Indent Style)

3 Vein stages

The vein is predominantly formed from massive milky white quartz, produced by multiple, sub–millimetre wide vein generations with minor pyrite, chalcopyrite, and galena. The multigenerational quartz has recrystallized, however, the form of the finer veinlets is preserved and can be distinguished through translucency and inclusion density variations in plane–polarised light. Through examining crosscutting relationships, textures and mineral associations, a detailed paragenesis has been determined (Spence–Jones 2013)(Fig. 1):

Stage 1 – early quartz veining

The majority (up to an estimated 70–80% by volume) of the multigenerational quartz breccia making up the vein formed early in its development and is classified as Stage 1. This comprises a milky white quartz dominated matrix–supported breccia. The clasts (up to ~80 cm) are composed of silicified host rocks that are significantly rotated in relation to the orientation of fabrics in the host lithologies. The quartz was originally formed by a multitude of fine 50–1000 µm stringer veins but has now recrystallized.

Stage 2 – early Au–Ag mineralisation

Coarse, up to 2 cm, euhedral cubic pyrite crystals occur within the early quartz veins in sulfide–rich pods that range in size from 1 cm to up to 30 cm. These pods are hosted within the quartz vein and also form 1–10 cm halos around altered clasts. This early euhedral pyrite is interpreted to have formed later than the Stage 1 quartz veinlets since the pyrite has not been crosscut by any of the quartz veinlets nor do they contain any [illegible] inclusions.

No space between paragraphs of same section

The coarse pyrite crystals host the earliest [illegible] (±Cu, Pb) mineralisation within fractures and as t[illegible] inclusions. The fractures contain the assemblage hessite + Au–Ag alloy + galena ± altaite ± chalcopyrite that is diagnostic of the Au–Ag mineralisation.

Stages 3–4 – evolution of the Au–Ag mineralisation

The vein material formed during Stages 1 and 2 is cross cut and comminuted by later narrow, 0.5–10 cm–wide shears that typically form anastomosing arrays up to half a metre wide. These shears host abundant chalcopyrite and galena with subordinate pyrite, sphalerite, calcite and Au–Ag alloy. The sulfides comprise >50% by volume of the late vein mineralogy. Stage 3 and 4 veins have been separated to represent end–members of a continuous trend based on the relative proportions of chalcopyrite and galena, progressing from 90% galena to 90% chalcopyrite (the latter often observed with calcite). The galena–rich veins are inferred to be earlier (Stage 3) as they are crosscut by later calcite–chalcopyrite veins. Whether a particular vein in an individual sample is Stage 3 or 4 is difficult to decide due to variations in mineralogy along the veins. The distinction is made for the deposit as a whole taking into account the compositions of the associated Au–Ag alloy, and the dominance of galena over chalcopyrite in the early Au–Ag mineralisation stages.

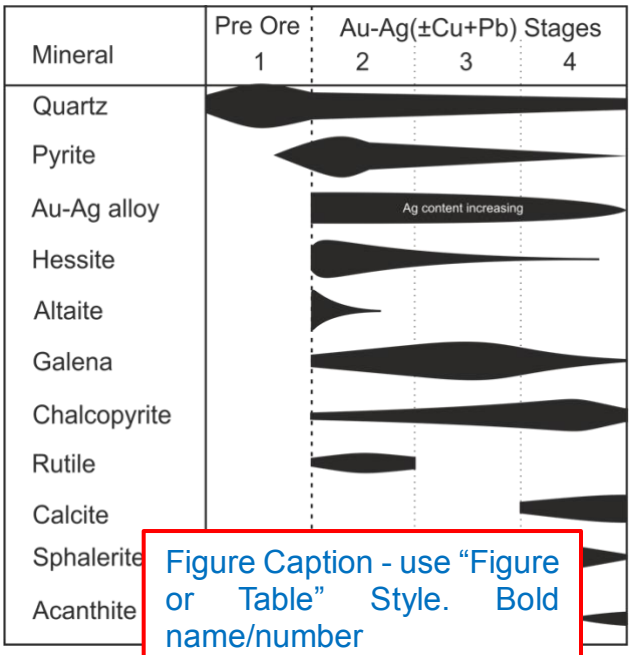

Figure Caption - use "Figure or Table" Style. Bold name/number

Figure 1. Paragenesis for the Cononish Au–Ag (±Cu, Pb) vein after Spence–Jones (2013).

4 Au–Ag alloy composition and association

The gold and silver concentrations in 215 individual Au–Ag alloy grains (formerly "electrum") were measured by SEM–EDX (Spence–Jones 2013). Compositions are highly variable, ranging from ~10% to ~90 wt.% Ag (Fig. 2). This is in contrast to many hydrothermal gold deposits, [illegible]ermal deposits, which show [illegible]nal ranges with Au–Ag alloy [illegible]Au, or 60–90% as reported [illegible] and Mortensen 2006, 2016; Chapman et al. 2010; Morrison et al. 1991).

Narrower ranges in composition (10–20% variation) occur within individual samples, indicating that the gold formed under similar conditions within a thin section sized sample of the vein. This supports the textural observations that later fluid phases have overprinted the earlier phases chemically and texturally, unless minerals are shielded from the late fluid as inclusions within early minerals.

There is a distinct association of the Au–rich alloy (gold) grains with hessite, whereas Ag–rich alloy (silver) is strongly associated with chalcopyrite (Fig. 2). Galena

DO NOT insert page numbers

is associated with the whole range of Au–Ag alloy compositions.

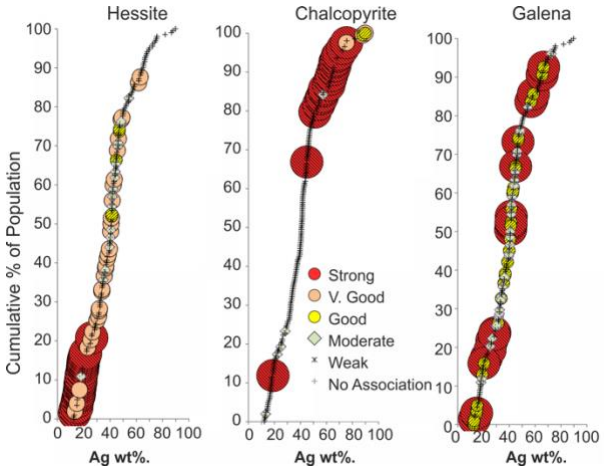

Figure 2. Composition of the Au–Ag alloy grains with observed mineral associations for hessite, chalcopyrite and galena using a qualitative scale. The size of the circle indicates the qualitative strength of the association: Strong association indicates the phases are clearly related, for example intergrown mineral textures. Moderate association indicates minerals that are observed together in a fracture or a veinlet. Weak association represents a tenuous link, such as Au–Ag alloy occurring in veins sets that contain the associated mineral distally. No association indicates the minerals were not observed with Au–Ag alloy in a vein.

Ensure text and detail on figures is readable at this size – text may need to be increased.
Note that figures can be two columns wide

5 Sulfur isotope data

Figure 3A shows 16 new pyrite S–isotope ar
with the combined published S–isotope dataset for Cononish. These show a range of $\delta^{34}S$ values from -1.9 to +11.4‰. Samples for this study were taken from coarse pyrite crystals that are temporally constrained in the paragenetic sequence described above. This reveals a trend of increasing $\delta^{34}S$ through the paragenetic sequence (Fig. 3B). Two samples that could relate to either Stage 3 or 4, as they show mineralogical and textural features of both stages, were plotted as Stage 3.5. To avoid bias in the results, the position of the samples in the paragenesis was determined and recorded prior to analys

Section Headings: Only first word capitalised (unless formal name)

Second order subsection (Heading 2 Style)

6 Discussion

6.1 Evolution of Au–Ag alloy composition

At Cononish, the Au–Ag alloy coexists with hessite, in which case the activity of Ag will be buffered by this phase (Gammons and Williams–Jones 1995) and the composition of Au–Ag alloy will thus be dependent on the activity of Te_2 in the system (Afifi et al. 1988). Put simply, if aTe_2 is high then large proportions of hessite will precipitate removing Ag available to the Au–Ag alloy and keeping the activity of Ag low. This will produce Au–rich alloy, as the buffered ratio of the Au/Ag activity will be high. In Stage 2, hessite is abundant along with Au–rich alloy; 90–75% Au. In Stages 3 and 4, the abundance of hessite decreases (Fig. 1), with no hessite seen in Stage

In text: figure X, or (Fig. X)

4, and here associated Au–Ag alloy grains have higher silver contents; 10%–75% Au. In late Stage 4 veinlets, acanthite occurs instead of hessite. It is interpreted that high aTe_2 in the early fluid controlled the composition of the early Au–Ag alloy and a progressive decrease in aTe_2 ely more Ag– n late Stage 4 Te_2 with time e would have would seem uid inclusion ly it relates to

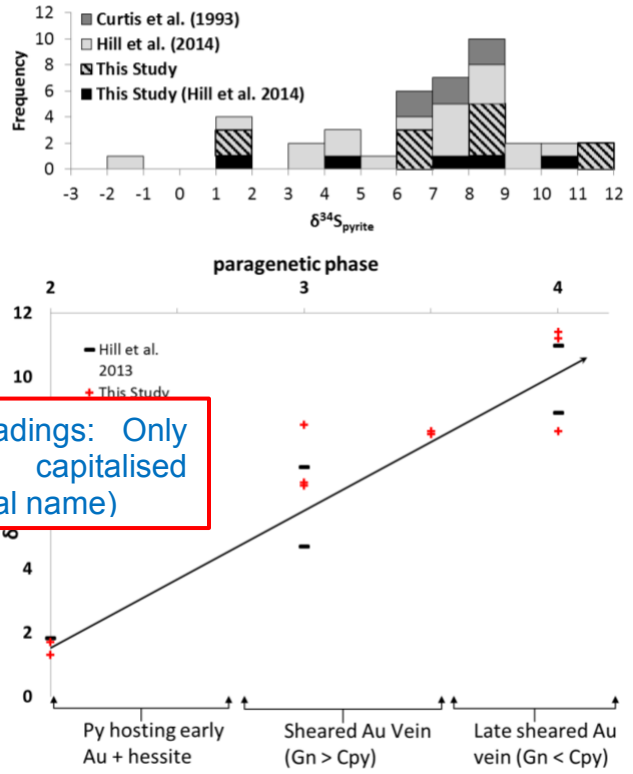

Figure 3. a. Histogram of compiled pyrite $\delta^{34}S$ for the Cononish deposit. **b.** Pyrite $\delta^{34}S$ vs. paragenetic stage.

6.2 Sulfur sources

The evolution in $\delta^{34}S_{pyrite}$ represents a significant shift in the sulfur isotope composition of the fluid, which is interpreted as a change of the sulfur source. Hill et al. (2013) examined the $\delta^{34}S$ of the local stratigraphy and discussed potential sulfur reservoirs. They demonstrated that it is possible to produce the full range of S–isotope values at Cononish, either from mixing of sulfur from different units in the local stratigraphy, or by mixing of magmatic sulfur with metasedimentary derived sulfur with $\delta^{34}S \geq +12‰$ from particular SEDEX–bearing stratigraphic units. Hill et al. (2013) advocated the latter scenario given the timing of the mineralisation long after metamorphism, but synchronous with the final stages of nearby granite magmatism and its mineralisation (Neilson et al. 2009). The paragenetically constrained pyrite $\delta^{34}S$

DO NOT insert page numbers

data support this interpretation, with the increase through the paragenesis interpreted as an early magmatic fluid progressively mixing over time with metasedimentary sulfur. To produce the same trend in $\delta^{34}S$ values over time from a purely metasedimentary–sourced hydrothermal system would have required mixing of fluids from different reservoirs that changed during deposit formation.

7 Implications

The Cononish Au deposit formed as the result of an early fluid pulse from a low–$\delta^{34}S$ (~1‰), high Te+Au+Ag source that evolved towards a high–$\delta^{34}S$ (≥11‰), low Te fluid with time. The low $\delta^{34}S$ source is interpreted here as a magmatic pulse of fluid and the evolution away from the strongly Te–saturated initial fluid is interpreted as a waning of magmatic fluid input and regaining of geochemical equilibrium with the Dalradian metasediments. Thus in *some* orogenic Au deposits it would seem that high Te relates to an input of magmatic fluid.

Acknowledgements

NH was funded by the Natural Environment Research Council (NERC) Open CASE studentship NE/H017755/1 with Scotgold Resources Ltd. Scotgold are acknowledged for financial and logistical field support and access to company information. S–isotope analyses were carried out at SUERC under NERC Isotope Facilities grant IP–1317–051[illegible] the Isotope Com[illegible] supported by NER[illegible] grant NE/M01084[illegible] and Supply (TeaSe[illegible]

References – use Reference List Style. Must comply with Mineralium Deposita standards and guidelines

References

Afifi AM, Kelly WC, Essene EJ (1988) Phase relations among tellurides, sulfides, and oxides; I, thermochemical data and calculated equilibria. Econ Geol 83:377–394.

Burrows DR, Spooner ETC (1989) Relationships between Archean gold quartz vein–shear zone mineralization and igneous intrusions in the Val d'Or and Timmins areas, Abitibi subprovince, Canada. Econ Geol Monograph 6:424–444.

Chapman RJ, Mortensen JK (2016) Characterization of gold mineralization in the northern Cariboo Gold District, British Columbia, Canada, through integration of compositional studies of lode and detrital gold with historical placer production: A template for evaluation of orogenic gold. Econ Geol 111:1321–1345.

Chapman RJ, Mortensen JK, Crawford EC, Lebarge W (2010) Microchemical studies of placer and lode gold in the Klondike district, Yukon, Canada: 1. Evidence for a small, gold–rich, orogenic hydrothermal system in the Bonanza and Eldorado Creek area. Econ Geol 105:1369–1392.

Craw D, Chamberlain CP (1996) Meteoric incursion and oxygen fronts in the Dalradian metamorphic belt, southwest Scotland: A new hypothesis for regional gold mobility. Miner Deposita 31:365–373.

Curtis SF, Pattrick RAD, Jenkin GRT, Fallick AE, Boyce AJ, Treagus JE (1993) Fluid inclusion and stable isotope study of fault–related mineralization in Tyndrum area, Scotland. Trans Inst Min Metall Section B–Appl Earth Sci 102:B39–B47.

Earls G, Patterson RTG, Clifford JA, Meldrum AH (1992) The geology of the Cononish gold silver deposit, Grampian Highlands of Scotland. In Bowden AA (ed) The Irish minerals industry 1980–1990, Irish Association for Econ Geol pp 89–103.

Gammons CH, Williams–Jones AE (1995) Hydrothermal geochemistry of electrum – thermodynamic constraints. Econ Geol 90:420–432.

Goldfarb RJ Groves DI (2015) Orogenic gold: Common or evolving fluid and metal sources through time. Lithos 233:2–26.

Goldfarb RJ, Hart C, Miller M, Miller L, Farmer GL, Groves DI (2000) The Tintina Gold Belt – A global perspective. In Tucker TL, Smith MT (eds) The Tintina gold belt – Concepts, exploration, and discoveries. British Columbia and Yukon Chamber of Mines Spec Vol 2:5–34.

Goldfarb RJ, Baker T, Dubé B, Groves DI, Hart CJR, Gosselin P (2005) Distribution, character, and genesis of gold deposits in metamorphic terranes. Econ Geol 100th Anniv Vol pp 407–450.

Groves DI, Goldfarb RJ, Gebre–Mariam M, Hagemann SG, Robert F (1998) Orogenic gold deposits: A proposed classification in the context of their crustal distribution and relationship to other gold deposit types. Ore Geol Rev 13:7–27.

Hill NJ, Jenkin GRT, Boyce AJ, Sangster CJS, Catterall DJ, Holwell DA, Naden J, Rice CM (2013) How the Neoproterozoic S–isotope record illuminates the genesis of vein gold systems: An example from the Dalradian Supergroup in Scotland. Geol Soc, London, Spec Pub 393:213–247.

Morrison GW, Rose WJ, Jaireth S (1991) Geological and geochemical controls on the silver content (fineness) of gold in gold–silver deposits. Ore Geol Rev 6:333–364.

Neilson JC, Kokelaar BP, Crowley QG (2009) Timing, relations and cause of plutonic and volcanic activity of the Siluro–Devonian post–collision magmatic episode in the Grampian terrane, Scotland. J Geol Soc 166:545–561.

Pattrick RAD, Boyce A, MacIntyre RM (1988) Gold–silver vein mineralization at Tyndrum, Scotland. Mineral Petrol 38:61–76.

Rice CM, Mark DF, Selby D, Hill NJ (2012) Dating vein–hosted Au deposits in the Caledonides of N. Britain. Trans Inst Min Metall (Section B. Appl Earth Sci) 121:199–200.

Science and Technology Committee, House of Commons (2011) Strategically important metals. HC 726, The Stationery Office Limited, London.

Scotgold Resources Limited (2015) Cononish gold project study update and JORC 2012 ore reserve estimate http://www.asx.com.au/asxpdf/20150526/pdf/42yt26kn3xqj6x.pdf.

Spence–Jones C (2013) Metallurgical investigation of ore at Cononish Gold Mine, Scotland. MGeol thesis, University of Leicester.

Stephenson D, Mendum JR, Fettes DJ, Leslie AG (2013) The Dalradian rocks of Scotland: An introduction. Proc Geol Ass 124:3–82.

Tanner PWG (2012) The giant quartz–breccia veins of the Tyndrum–Dalmally area, Grampian highlands, Scotland: Their geometry, origin and relationship to the Cononish gold–silver deposit. Earth and Environ Sci Trans Roy Soc Edinburgh 103:51–76.

Tanner PWG (2014) Structural controls and origin of gold–silver mineralization in the Grampian terrane of Scotland and Ireland. Geol Mag 151:1072–1094.

Tanner PWG, Thomas PR (2010) Major nappe–like D2 folds in the Dalradian rocks of the Beinn Udlaidh area, Central Highlands, Scotland. Earth and Environ Sci Trans Roy Soc Edinburgh 100:371–389.

Wyman DA, Cassidy KF, Hollings P (2016) Orogenic gold and the mineral systems approach: Resolving fact, fiction and fantasy. Ore Geol Rev 78:322–335.

DO NOT insert page numbers